

INVESTIGATING THE GROUND ENERGY DISTRIBUTION OF PARTICLES PRODUCED IN EXTENSIVE AIR SHOWERS

Itab F. Hussein^{1a*} and Al-Rubaiee A. A^{2a}

Mustansiriyah University, Department of Physics, College of Science, Baghdad, IRAQ. E-mail: itabfadhil@uomustansiriyah.edu.iq¹; dr.rubaiee@uomustansiriyah.edu.iq²

Corresponding author: itabfadhil@uomustansiriyah.edu.iq

Received: 22th Jul 2021

Accepted: 22th Dec 2021

Published: 30th Jun 2022

DOI: <https://doi.org/10.22452/mjs.vol41no2.6>

ABSTRACT The energy spectra of particles arriving at the ground is a significant observable in the analysis of extensive air showers (EAS). Energy distributions at ground were studied for primary particles (¹²C, ⁵⁶Fe, p, and ²⁸Si) with high primary energies (10^{17} , 10^{18} , 10^{19} , and 10^{20} eV) from two zenith angles (0° and 30°). 960 EAS were simulated using the Monte-Carlo program Aires (version 19.04.00) with three models of hadronic interaction (EPOS-LHC, QGSJET-II-04, and Sibyll2.3c). Good agreement was obtained by comparing the present results with results simulated using CORSIKA for primary iron at an energy of 10^{20} eV. In this study we investigated various secondary particles that arrive at the ground and deposit a portion of their energy on ground detectors. These results show that the distinction in energy distribution at ground is greater for primary protons than carbon, iron, or silicon nuclei at higher energies and steeper zenith angles.

Keywords: UHECRs, extensive air showers, energy at ground, AIRES Simulation

1. INTRODUCTION

When ultra-high energy cosmic rays (UHECRs) enter the Earth's atmosphere, they initially interact with oxygen or nitrogen molecules in the air, resulting in complex interactions and cascades that produce extensive air showers (EAS) containing hundreds of trillions of particles (Blümer, Engel, & Hörande, 2009; Knapp, 2003; Dongsu Ryu & Kang, 2011). Original particle characteristics, such as energy, direction of arrival, and element are derived by detection of secondary particles that reach the ground. Primary particles, which collide with the ground at high energies, are not directly detectable. A cascade of particles is released when they collide with the atmosphere, which is detected by telescopes and ground

equipment. From the detected shower indicator, the characteristics of this primary particle can be recreated (Aab, 2014; Bellido, 2017; Al-Rubaiee, Jassim, & Al-Alawy., 2021). In EAS, only a small percentage of secondary particles make it to the ground. Ground detectors, such as water Cherenkov tanks or scintillation detectors, collect a portion of the energy emitted by these particles (Hillas, 1971). Ionization and bremsstrahlung are two processes that cause electrons and muons to lose energy. Ionization is the primary source of energy loss for muons. Bremsstrahlung does not cause significant energy losses until muon energies in the thousands of GeV are reached. For electrons, on the other hand, bremsstrahlung does result in energy loss for particles with moderate starting energies (Sciuttu, 2002).

Models of hadronic interaction play a significant role in the estimation of EAS features. Alternatively, different models used in the AIRES simulation code have introduced phenomenological methods. The aim of the present work was to study the energy distribution at ground (E_{ground} ; i.e., the total energy deducted from the rest-mass energy) (Drescher, 2003) for electrons, muons, and pions by several models of hadronic interaction usually applied to air shower simulation. These included EPOS-LHC (Pierog, 2015), QGSJetII.04 (Ostapchenko, 2011), and Sibyll2.3c (Ahn, 2009). These models have the best representation of high-energy hadronic interactions (Klages, 1997).

2. ENERGY ESTIMATION VIA HEITLER AND MATTHEWS MODELS

On a microscopic level, simple cascade models offer some insight into the relationship between air shower observables and interaction physics (Matthews, 2001; Pierog, 2006; Heitler, 1954). Heitler's model of particle cascades can be used to define the major aspects of electromagnetic shower profiles (Matthews, 2005; Alvarez-Muniz, 2002). Assume that a particle (electron, positron, or photon) divides its energy (E_o) evenly into two separate particles, after traveling X_o radiation length in the air, and allows secondary particles to frequent this process as shown in Figure 1:

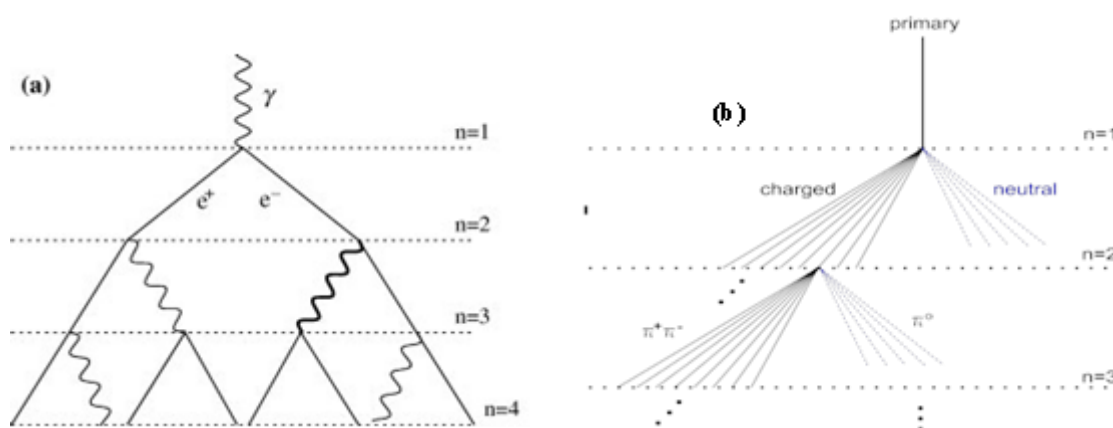


Figure 1. Diagrammatic views of (a) an electromagnetic Heitler model & (b) Hadronic Heitler-Matthews model (Matthews, 2001; Aartsen, 2013).

The result is a particle cascade after n radiation durations that has included into ($N = 2^n$) and energy equal ($E = E_o/N$). Multiplication stops when the particle energies are too low for pair

production or bremsstrahlung. This energy is referred to the critical energy (E_c^{em}). At this point, maximum particle number is attained, known as (N_{max}). When the energy of all particles is the same, then:

Since
$$E_o = E_c^{em} \cdot N_{max} \quad \text{----- (1)}$$

$$(N_{max} = 2^{n_{max}}) \quad \text{----- (2)}$$

Where
$$n_{max} = \ln\left(\frac{E_o}{E_c^{em}}\right) \cdot \frac{1}{\ln 2} \quad \text{----- (3)}$$

From Eq. (3), (N_{max}) is directly proportional to the primary energy E_o (

Linsley, 1977). EAS was first modeled on protons by Matthews following a method

similar to Heitler's. Charged pions (N_{ch}) and neutral pions ($\frac{1}{2} \cdot N_{ch}$) are produced when protons traverse one interaction length and interact, which decays into

photons, immediately beginning an electromagnetic shower. As for the electromagnetic cascade, during particle production we assume the same energy split. Following n interactions:

$$N_{\pi} = (N_{ch})^n \text{----- (4)}$$

The total energy of the charged pions produced is $(\frac{2}{3})^n \cdot E_o$. After n interactions, the energy per charged pion is:

$$E_{\pi} = \frac{E_o}{(3/2N_{ch})^n} \text{----- (5)}$$

The process ends when the energy of pions falls under the critical energy (E_c^{π}), and they decay into muons. The muon's number is

($N_{\mu} = N_{\pi} = (N_{ch})^{n_{max}}$), where n_{max} is the number of interaction lengths needed to exceed the interaction length of the charged pion:

$$n_{max} = \frac{\ln(\frac{E_o}{E_c^{\pi}})}{\ln(\frac{3}{2N_{ch}})} \text{----- (6)}$$

Therefore, the entire energy is split into two electromagnetic and hadronic channels.

$$E_o = E_c^{e.m.} \cdot N_e + E_c^{\pi} \cdot N_{\mu} \text{----- (7)}$$

The muon number is thus reliant on the secondary hadronic abundance and pion charge ratio. According to Matthews' model, energy is provided by a linear combination of the electron and muon sizes. This finding is unaffected by transitions in energy separated between the electromagnetic and hadronic channels, and it is unaffected by the parent particle's mass (Bergmann, 2007).

3. SIMULATION OF EAS USING THE AIRES SYSTEM

Extensive shower simulations using the program AIRES ("AIR-shower Extended Simulations") version (19.04.00) is a Monte-Carlo simulation program. There were four atomic nuclei to consider: carbon, iron, proton, and silicon with energies of 10^{17} , 10^{18} , 10^{19} and 10^{20} eV

and zenith angles of 0° and 30° . Ground level was simulated at 1400 m above the equivalent sea level to yield a slant depth of 1000 g/cm^2 . Cut energies for gamma photons, electrons, muons, and mesons were 80 KeV, 80 KeV, 10 MeV, and 60 MeV, respectively, and the energy of thinning algorithm was set to ($\epsilon_{th}=10^{-6}$). Additionally, the effect of three models of hadronic interaction (QGSJetII.04, EPOS-LHC, and Sibyll2.3c) on the energy distribution at ground of secondary charged particles produced in the EAS was considered.

4. RESULTS AND DISCUSSION

Secondary particles like electrons, muons, and pions carry the vast majority of the energy in EAS to the ground. Figures (2, 3 and 4) show particle number as a function of energy distribution of secondary particles at the ground in EAS of C, Fe, p, and Si primaries with energies of 10^{17} , 10^{18} , 10^{19} , and 10^{20} eV and zenith angles of 0° and 30° simulated using three different hadronic models (EPOS-LHC, QGSJET-II-04, and Sibyll2.3c respectively).

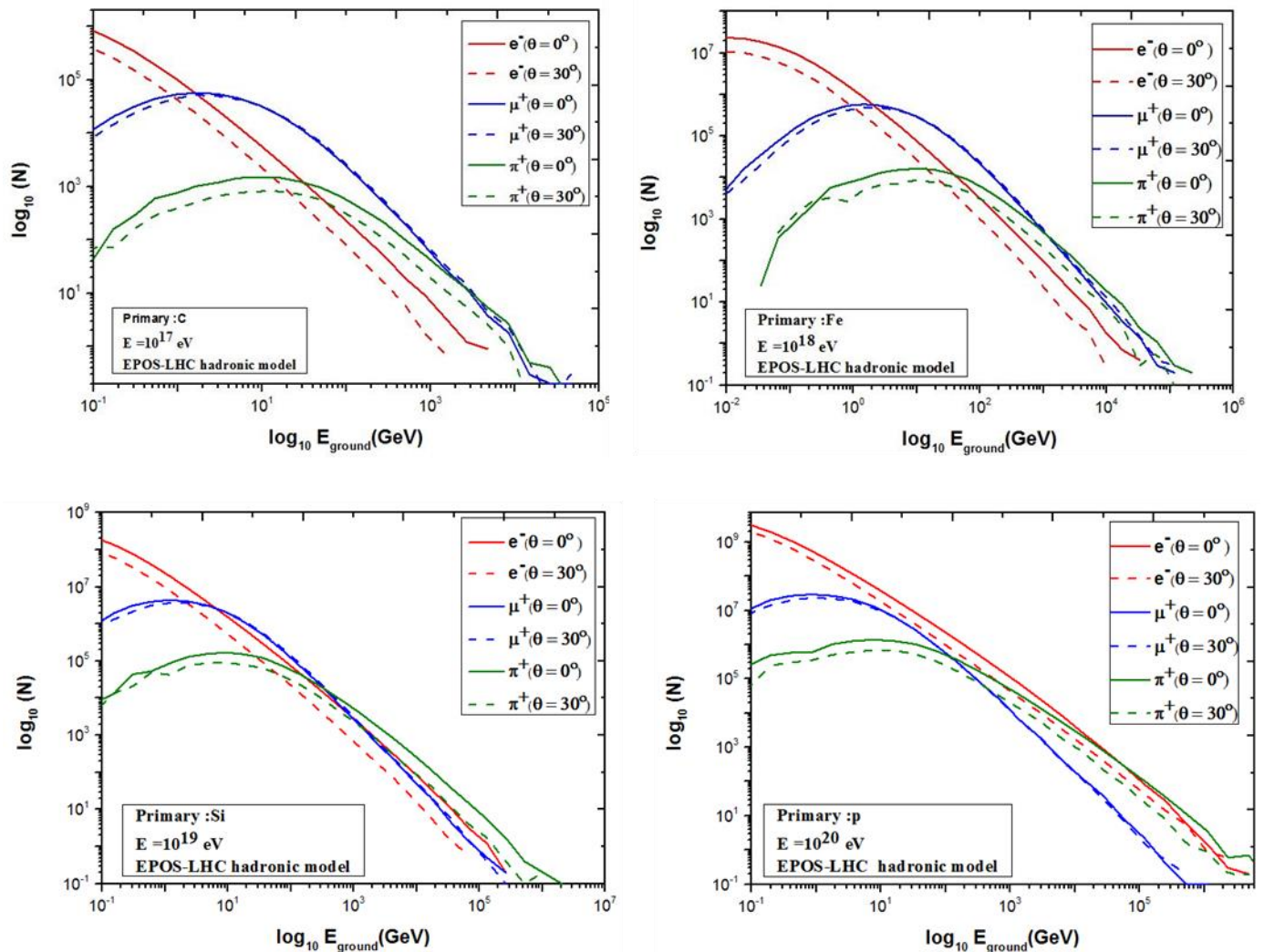


Figure 2. The number of secondary particles as a function of the energy distribution at ground for various primary particles and various energies for: vertical showers (solid lines) and inclined showers (dashed lines) using the EPOS-LHC hadronic model.

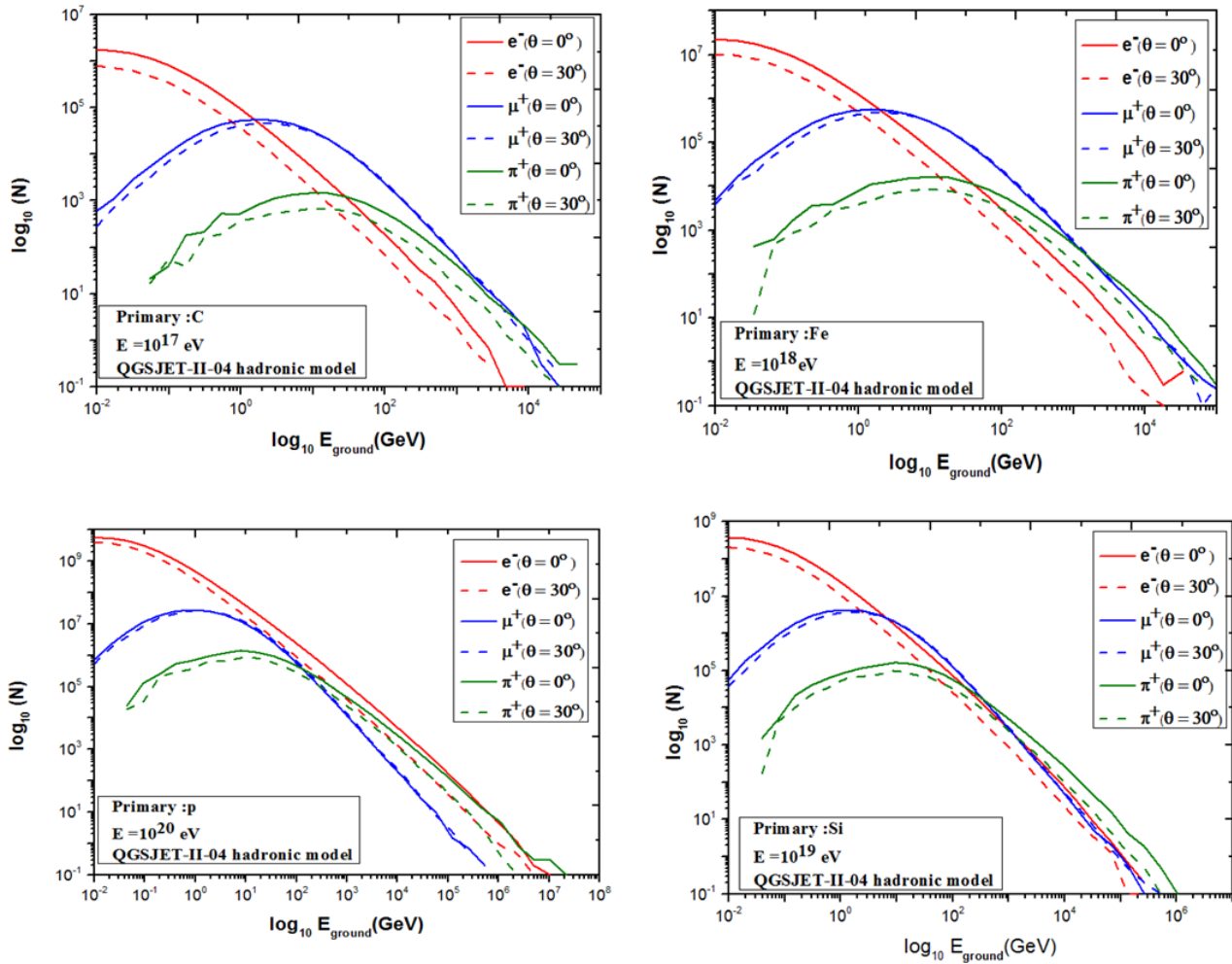


Figure 3. The number of secondary particles as a function of the energy distribution at ground for various primary particles and various energies for: vertical showers (solid lines) and inclined showers (dashed lines) using the QGSJET-II-04 hadronic model.

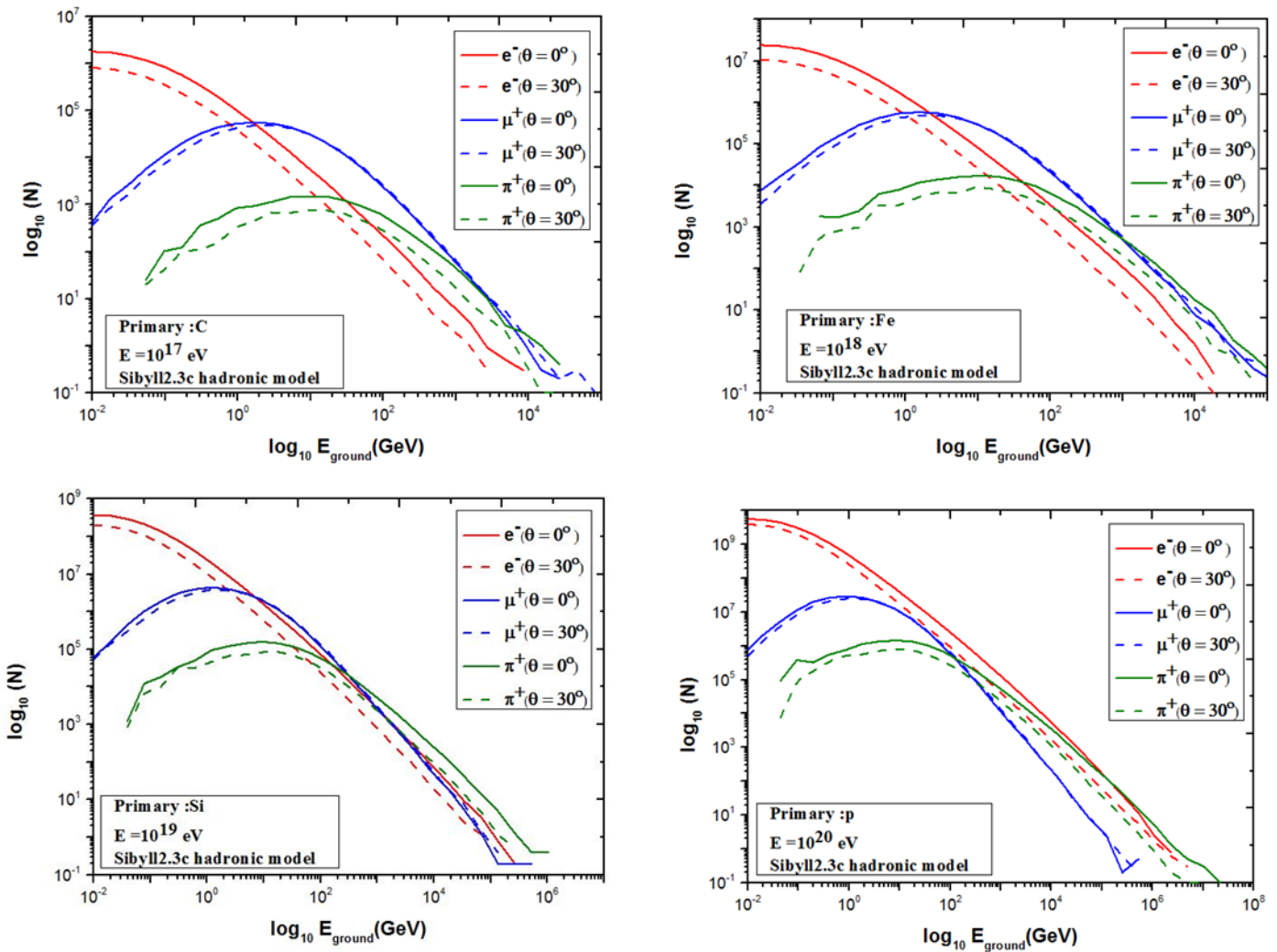


Figure 4. The number of secondary particles as a function of the energy distribution at ground for various primary particles and various energies for: vertical showers (solid lines) and inclined showers (dashed lines) using the Sibyll2.3c hadronic model.

As shown in figures (2, 3 and 4) the primary particle energy was proportional to the number of secondary particles and $N_{\text{electrons}} \gg N_{\text{muons}} \gg N_{\text{pions}}$ for all the cases that were simulated. Electrons and muons have widely different energies, with muons typically having GeV energies while electrons have MeV energies. This difference mostly originates from their disparate parentage, but also from the fact that muons suffer much lower scattering than electrons and thereby lose less energy to particles in the atmosphere (Sciuttu, 2002). We also note that greater amounts of particles did not necessarily indicate greater

energy; this is especially obvious for muons. Additionally, an important aspect was inclined showers; it is clear that particle number decreased when the EAS was inclined, since cosmic radiation is primarily isotropic. However, when the zenith angle rose, air absorption reduced the number of showers. This increased absorption more than offset the larger angle's effect. This was due to the inclined EAS having an effective length through the atmosphere as altitude over the $\cos\theta$, where θ refers to the zenith angle and altitude is the length from ground to the interaction point of the primary particle. Due to this

longer effective length, EAS had more time to develop and therefore looked "older" when it hit ground. The EAS maximum, the point in the development where the EAS had the most particles, was some way up in the atmosphere regardless of primary energy. After that point, the number of particles decreased. Figure (5) shows the energy spectra of electrons for primary particles C, Fe, p, and Si at the fixed primary energy 10^{17} eV and zenith angles of 0° & 30° , simulated using QGSJET-II-04, EPOS-LHC, and Sibyll2.3c hadronic

models. From this figure, it's clear that small variances were apparent between number of particles for the primary particles, while the behavior of protons were more distinctive compared to the other elements. That was due to the relative abundance of protons, since in the development of the showers, the parameter that drove the number of interactions and energy losses was quantity of material that the particles in the EAS spread across the atmosphere.

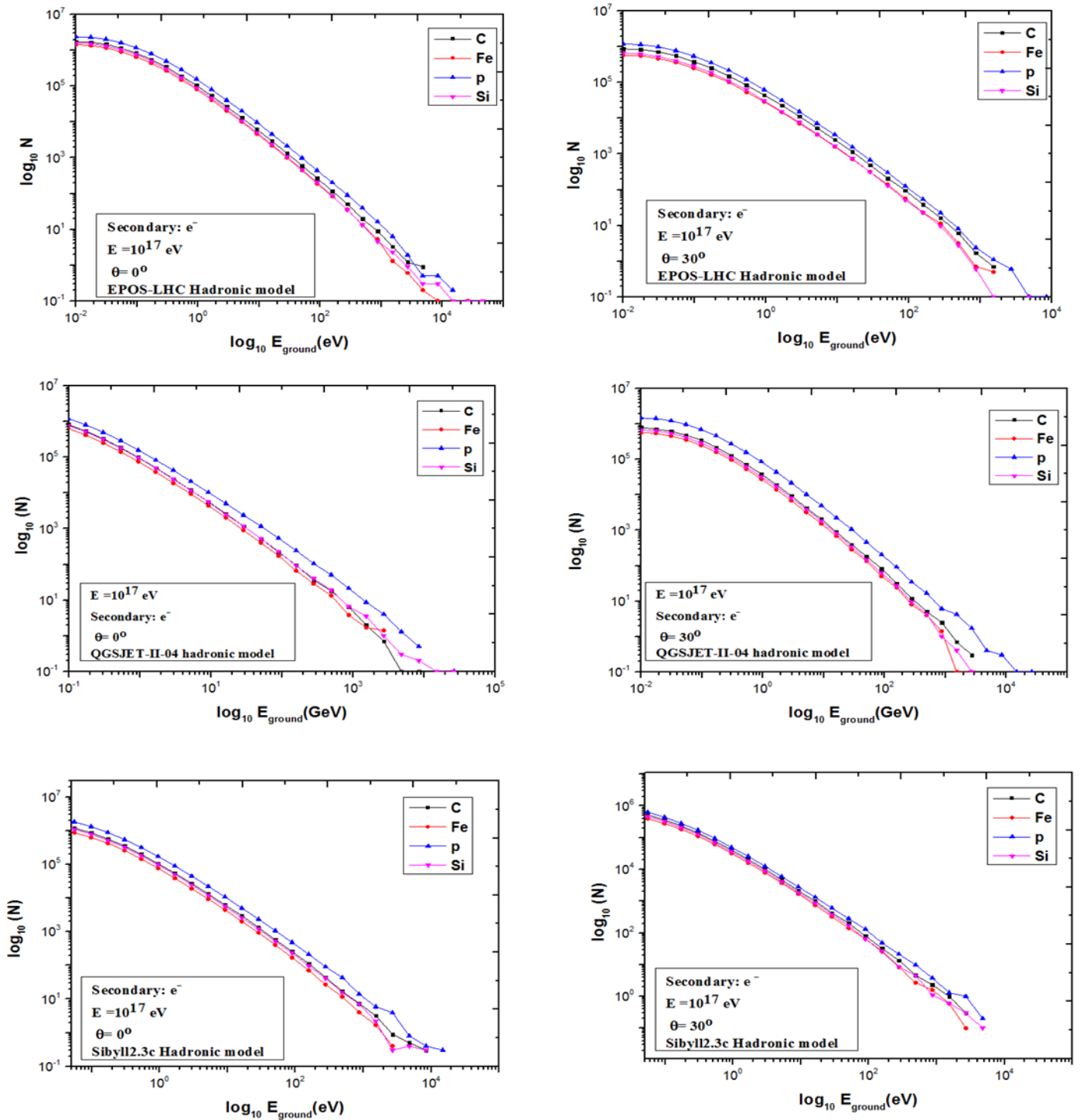


Figure 5. Number of electrons as a function of the energy distribution at ground for various primary particles at 10^{17} eV for vertical showers and inclined showers, simulated using EPOS-LHC, QGSJET-II-04, and Sibyll2.3c hadronic models.

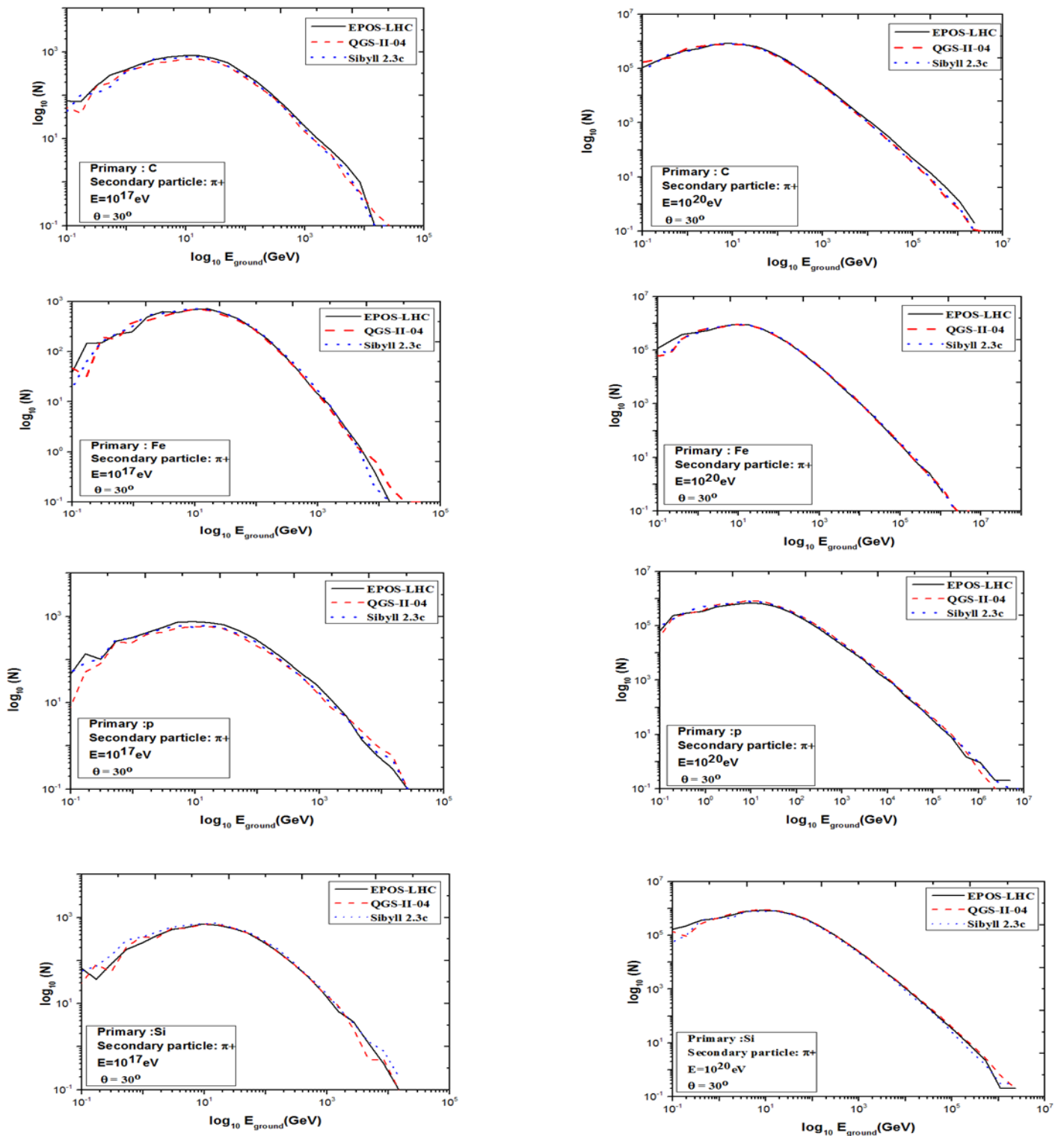


Figure 6. The simulation of energy distributions for various primary particles (C, Fe, p, and Si) and pion secondary particles using three models of hadronic interactions (EPOS-LHC, QGSJetII.04, and Sibyll2.3c) at the energies 10^{17} and 10^{20} eV with inclined showers ($\theta=30^\circ$).

The simulation of energy distributions is shown in Figure (6) for primary particles C, Fe, p, and Si, and pion secondary particles using three models of

hadronic interaction (EPOS-LHC, QGSJetII.04, and Sibyll2.3c) at energies 10^{17} and 10^{20} eV with $\theta=30^\circ$. Each type of line represents simulations carried out

using a particular model of hadronic interaction regarding the energy distribution at the ground. The distinction between the three models was relatively small, and in each of the three hadronic interaction models the quantity of secondary particles was similar, not completely different compared to the data but it added some technical improvements.

Figure (7) shows the comparison between the present results of energy distribution at ground performed by AIRES simulation (dash lines) and the CORSIKA simulation result (solid lines) (Soonyoung R.,2013). This figure displays good agreement for the muon-secondary particles initiated by primary iron with energy 10^{20} eV at a vertical zenith angle.

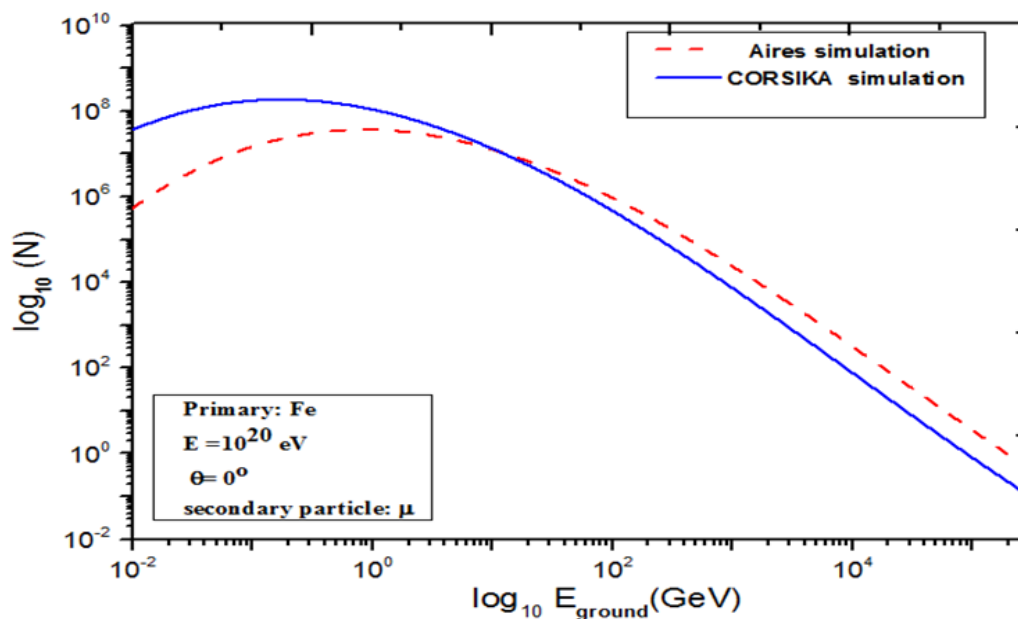


Figure 7. Comparison between the results of energy distribution at ground simulated by AIRES system and CORSIKA simulation. Result for primary iron at energy 10^{20} eV for muon secondary particles.

5. CONCLUSIONS

The simulation of EAS represents a large part of the studies used to study UHECRs for predicting Earth's energy distribution and elementary particle composition. In the present work, three hadronic models in AIRES simulation were compared through the distribution of particle energies on Earth. The results showed a discrepancy in the number and energies of particles that reach Earth, where the proton, which has a greater initial energy and a vertical EAS, had a clearly different behavior when compared to the

rest of the particles. The three hadronic interactions models used yielded very similar results. Such an agreement should be a major achievement, as it increases confidence that the behaviors of particles passing through Earth's detectors are being accurately simulated.

6. ACKNOWLEDGMENTS

The authors are grateful for help from the Mustansiriyah University in Baghdad-Iraq, and the designers of the Aires system.

7. REFERENCES

- Aab A. et al. [Pierre Auger Collaboration], Depth of maximum of air-shower profiles at the Pierre Auger Observatory. I. Measurements at energies above $10^{17.8}$ eV, Phys. Rev. D vol.90, no. 12, (2014).
- Aartsen M.G., et al, Measurement of the cosmic ray energy spectrum with IceTop-73, Phys. Rev. D88, 042004, (2013).
- Ahn E. J., et al., Cosmic ray interaction event generator Sibyll 2.1, Phys. Rev. D80, 094003 (2009).
- Al-Rubaiee A. A., J. Astrophys. Astr., 35, pp. 631–638(2014).
- AL-Rubaiee A. A., Jassim H.A.,and Al-Alawy I. T., J. Astrophys. Astr., pp.42, 52(2021)
- Alvarez-Muniz J., et al., Hybrid simulations of extensive air showers, Phys. Rev. D66, 033011 (2002).
- Bellido J. [Pierre Auger Collaboration], Depth of maximum of air-shower profiles at the Pierre Auger Observatory: Measurements above $10^{17.2}$ eV and Composition Implications, PoS ICRC (2017).
- Bergmann T., et al, One-dimensional Hybrid Approach to Extensive Air Shower Simulation, Astropart. Phys. 26, 420 (2007).
- Blümer J., Engel R., Hörandel J. R., Cosmic Rays from the Knee to the Highest Energies, Prog. Part. Nucl. Phys. 63, 293 (2009).
- Heitler W., "The Quantum Theory of Radiation" (Oxford University Press) (1954).
- Hillas A. M. et al., Proc. 12th ICRC 3,pp.1001-1006, (1971).
- Joachim Drescher H., et al., Model Dependence of Lateral Distribution Functions of High Energy Cosmic Ray Air Showers, astro-ph/0307453v2, (2003).
- Klages H. O., for the KASCADE Collaboration, The status of the extensive air shower experiment KASCADE Proc.25th ICRC.,6, pp-141-144, (1997)
- Knapp J. et al. Extensive air shower simulations at the highest energies, Astropart. Phys. 19, pp77-99, (2003).
- Linsley J., Proceedings of 15th ICRC (Plovdiv)8, pp, 207-210(1977).
- Matthews J., A Heitler model of extensive air showers, Astropart. Phys. 22 pp387-397, (2005).
- Matthews J., Energy Flow in Extensive Air Showers, Proc. 27th ICRC, Hamburg, p. 261, (2001).
- Ostapchenko S., Monte Carlo treatment of hadronic interactions in enhanced Pomeron scheme: I. QGSJET-II model, Phys. Rev. D. 83, 014018 (2011).
- Pierog T., et al., EPOS LHC: test of collective hadronization with LHC data, Phys. Rev. C. 92, 034906(2015).
- Pierog T., et al., Impact of Uncertainties in Hadron Production on Air-Shower Prediction, J. Phys. 56, A161 (2006).
- Renyi Ma, Dongsu Ryu & Hyesung Kang, J. Astrophys. Astr., 32, pp. 301–302, (2011)

Sciuttu S.J., AIRES user's guide and reference manual, version 2.6.0. La Plata, Argentina, (2002).

Soonyoung R. et al., Astroparticle Physics, Vol. 44, pp. 1-8, (2013)